ASTRO-2023-C017(080)

ALGEBRAIC AND SIMULTANEOUS ESTIMATION OF ATTITUDE MOTION AND INERTIA PROPERTIES

「画像に基づく角運動量ベクトルと慣性テンソルの同時推定」

Junichiro Kawaguchi[1], and Tetsuya Kusumoto[2]

Australian National University, University of Tokyo

Approaching to Target in Active Debris Removal (ADR)

The removal servicer should approach from the safe & appropriate direction.

The most important property is the Angular Momentum Vector, around which the markers move around.

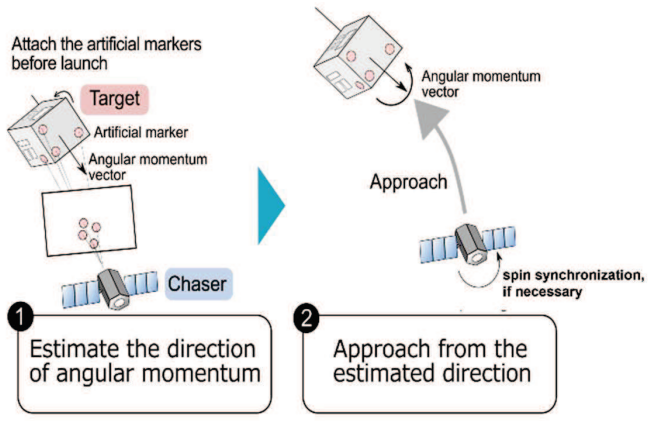

Fig.2 Approach Strategy to Uncooperative Target

Inertia tensor must be estimated to this end. It is difficult.

The inertia tensor may have varied from the original owing to the unbalanced fuel consumption or some corruption or fragmentation.

In case the robot fails to grab the debris, the debris motion is re-excited by the contact. And the estimation becomes more difficult.

Approaching to Target in Active Debris Removal (ADR)

Filtering is common and a large number of studies have been reported. However, they function only along with the reference trajectory and require a priori shape and inertia properties. So, such an approach is applicable for cooperated target.

They do not work for the debris whose shape and inertia properties have significantly been altered.

When the servicer spacecraft hits the target debris, another motion starts, and filters can never function.

Filtering or Algebraic Approaches. Prescribed Targets are requested on Debris or not.

The authors have dealt with the problem for decades.

However, the solution has not been simply obtained despite a huge amount of research.

Filters do not function robustly as noted.

This paper presents a new batch estimation method for both the attitude motion and the inertia properties at the same time, excluding reliance on the a priori information.

Mathematically speaking, the estimation of the inertia tensor results in solving the corresponding Lyapunov matrix equation.

The method does not request the debris to carry some prescribed target markers on it at launch.

It has only to rely on the shape information of some parts onboard the debris based on the drawings left, when the debris needs to be removed actually.

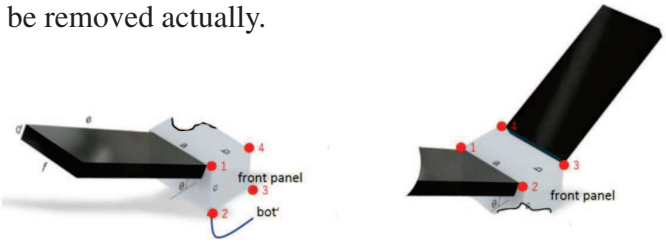

Fig.7 Fragmented Debris and markers constituting a shape

“衛星回収を目的とした宇宙用マニピュレータの制御”, 二宮, 中谷, 川口, 播磨, 宇宙科学技術連合講演会講演集, pp. 250-251, 1988.

タンブリング衛星の自律的回収のための視覚情報処理, 第34回宇宙科学技術連合講演会講演集 446-447, 1990

スライディングモード型制御を用いた宇宙用マニピュレータの制御, 播磨 浩一, 川口 淳一郎, 中谷 一郎, 二宮 敬虔, 日本ロボット学会誌、1991 年 9 巻 5 号 p. 572-579

日本航空宇宙学会誌 第 42 巻 第 490 号 (1994 年 11 月)

一論 文一

宇宙用マニピュレータを用いた衛星捕捉制御*1

Control Scheme for Retrieval of Tumbling Satellite by Space Manipulator

永 松 弘 行*2・久 保 田 孝*2
Hiroyuki NAGAMATSU, Takashi KUBOTA
中 谷 一 郎*2
and Ichiro NAKATANI

Key Words: Space Manipulator, Autonomous Satellite Retrieval, Visual Control, Hardware Simulator

Abstract

This paper describes a practical control scheme for autonomous retrieval of tumbling satellite with an onboard manipulator using a CCD camera. In the retrieval of a satellite, a reference trajectory for positioning the end-effector of manipulator is generated with time delay because of processing time for target motion estimator and manipulator controller. Consequently, the end-effector fails to capture the target, and the control system shows poor performance. To solve this problem, a control system is proposed, which utilizes predictive trajectory based on target satellite dynamics. The validity and the

タを制御するフェーズ(Phase II)とからなる．Phase Iに関する研究では，マニピュレータは推定結果に基づいて完全に制御されることを前提としている[2] Phase IIに関する研究では，視覚センサの雑音や画像処理に伴う時間遅れ，制御系の遅れなどは，完全に補償されていることを前提としており[3]，運動推定系の処理時間を考慮したものはあまりない 運動推定系をむだ時間系とみなして，ビジュアルフィードバック系の安定性を考察した研究[4]もあるが，この場合はマニピュレータ制御系は理想的なものとして扱っている．しかし，実用という点を考慮すると，これら二つ

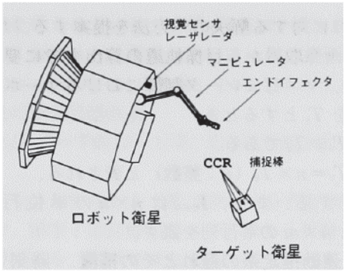

第 1 図 衛星回収の概念

2.2 **TS の運動式** 捕捉の対象となる TS は，宇宙空間ではタンブリング運動をし，その運動解析は複雑である．ここでは，視覚センサとして RS 本体に固定された単眼の CCD (Charge Coupled Device) カメラを考える．また，TS はほぼ立方体で，最大慣性主軸上には捕捉棒が取り付けられている．捕捉棒が取り付けられた捕捉面上で，TS の重心・慣性主軸との関係が既知である特徴点として，4 つの CCR (Corner Cube Reflector) を考える．RS からレーザ光を照射し，CCR からの反射光をカメラ画像面上で求める．それらを観測値として拡張 Kalman フィルタ (Extended Kalman Filter : EKF) を適用し，Σ_t における TS の位置・姿勢を推定する．

日本ロボット学会誌 Vol. 12 No. 3, pp. 444～450, 1994

技術論文

フリーフライングロボットによる視覚情報を用いたターゲットの捕獲

下 地 治 彦*1 井 上 正 夫*1 土 屋 和 雄*2
中 谷 一 郎*3 川 口 淳一郎*3 二 宮 敬 虔*3

Satellite Grappling by Free-Flying Robot Based on Visual Information

Haruhiko Shimoji*1, Masao Inoue*1, Kazuo Tsuchiya*2,
Ichiro Nakatani*3, Jun'ichiro Kawaguchi*3 *and* Keiken Ninomiya*3

This paper deals with a free-flying space robot which grapples a target satellite based on a visual feedback control scheme. As the robot body is not fixed in an inertial space, manipulator motion causes changes in the view of the visual sensor. Therefore the closed loop system for the manipulator controller involves the visual data processing which normally takes long calculation time. We construct a control system which is not explicitly affected by the calculation time and analyze stability of the system. Analysis results show that a stable control system can be constructed in spite of the long calculation time, on condition that the manipulator trajectory which is not close to singular points is settled. Moreover we developed a zero gravity motion simulator which combined a computer simulation and servo mechanisms. An experimental space robot system is constructed and experiments to grapple a target are performed on the simulator. It is confirmed through the experiments that the free-flying space robot automatically grapples the target with the visual feedback control scheme proposed.

Key Words: Free-Flying Space Robot, Visual Feedback, Satellite Grappling, Stability, 0-g Motion Simulator

4.2 宇宙ロボットシステム

(1) ハードウェアの構成

ロボットは，1 個のマニピュレータと 2 個の CCD カメラからなる．

マニピュレータは全長約 1[m]で 7 自由度である．各関節は

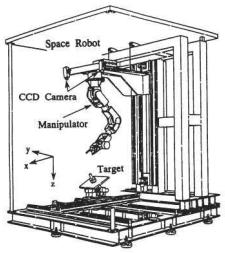

Fig. 10 6-Axis zero gravity simulation system

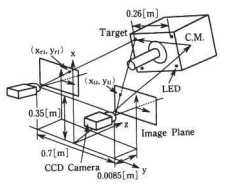

Fig. 11 Image coordinate system

タを制御する．

ターゲットのモデルは既知とする．計測精度を高めるために，拡張カルマンフィルタを用いて画像中の LED 像の位置からターゲットの位置と姿勢を算出する．

状態ベクトルは，

$$\boldsymbol{x}=[\boldsymbol{r}_o, \boldsymbol{p}, \dot{\boldsymbol{r}}_o, \dot{\boldsymbol{p}}]^T \in \boldsymbol{R}^{12} \quad (10)$$

とした．ここで，$\boldsymbol{r}_o$, $\boldsymbol{p}$ はそれぞれターゲットの重心位置ベクトルとオイラー角を表す．

観測ベクトルは，

$$\boldsymbol{z}=[\cdots, x_{li}, y_{li}, \cdots, x_{ri}, y_{ri} \cdots]^T \in \boldsymbol{R}^{m+n} \quad (11)$$

とした．$(x_{li}, y_{li}), (x_{ri}, y_{ri})$, m, n はそれぞれ左右の画像中の LED 像の座標，認識された個数で，m と n は入力された画像に応じて増減する．幾何学的に位置と姿勢を算出した結果を観測ベクトルとする方法に比較すると，式(11)の観測ベクトルを用いると複数の特徴点の情報を適切な重みで評価できるし，マニピュレータの動作中にいくつかの LED 像がマニピュレータの影になった場合，観測ベクトルと対応する行列の次数を変えるだけで処理方式自体は変更せずに対応できるという利点がある．

ダイナミクスモデルは，本来マニピュレータの動作反力によるロボットボディの運動も含めなければならないが，計算負荷を軽減するため，ロボットボディは固定され，ターゲットのみ自由運動するとした．この場合ロボットボディの運動はダイナミクスモデルのエラーとなるが，マニピュレータの運動速度が大きくない場合には安定した計測が可能である．また，観測モデルは透視変換を表す．

ダイナミクスモデルと観測モデルはいずれも非線形となるので，拡張カルマンフィルタを構成した．

(3) 視覚認識（フィルタ出力の補正）

拡張カルマンフィルタを用いることによって，カメラ座標系における計測精度は高められるが，マニピュレータの取り付け誤差や関節角度の初期化の誤差は除去できない．

本研究では，マニピュレータのハンドに取り付けられた LED を視野内に捕えることによりハンドの位置を計測し，これと関節角度から計算されるハンドの位置を比較することによ

Pose Estimation Fundamentals

Here is introduced a pin-hole camera as below.

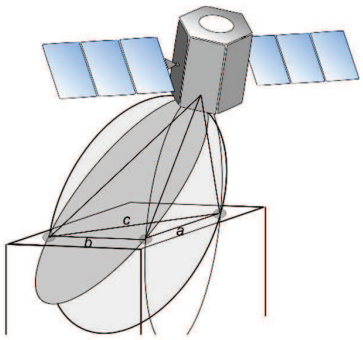

Fig.4 Schematic observation of markers

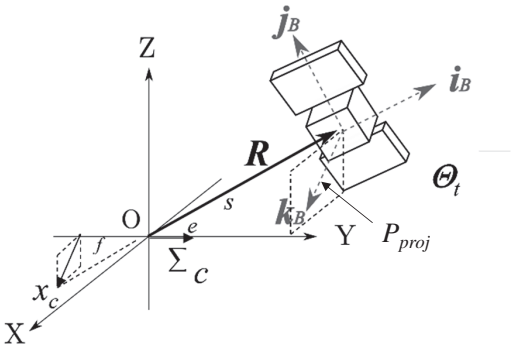

Fig.3 Camera & Body fixed frames

$$P_{proj} = (1 - ee^T)R. \tag{1}$$

It corresponds to the pixel position vector x_c on the focal plane. As a result, the unit vector i from the origin to each marker is obtained as

$$i = (-fe + x_c)/|-fe + x_c|. \tag{2}$$

When the slant range s becomes available, the position vector is expressed as

$$R = -si. \tag{3}$$

Basics: 'Pose Estimation' : Four Markers are required in general.

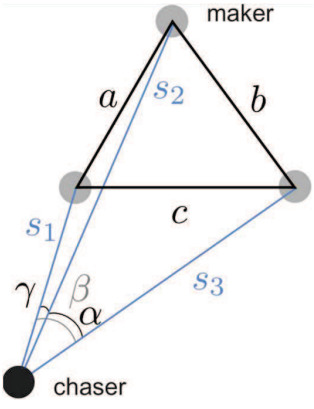

Fig.5 Pose estimation via three markers

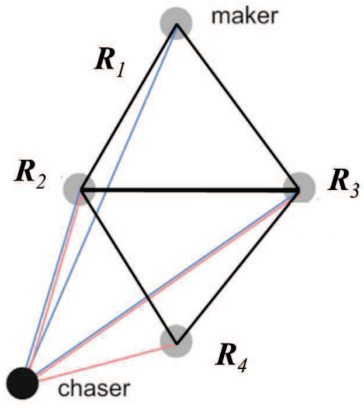

Fig.6 Pose estimation via four markers

$$s_2^2 + s_3^2 - 2s_2s_3\cos\alpha = a^2$$
$$s_1^2 + s_3^2 - 2s_1s_3\cos\beta = b^2$$
$$s_1^2 + s_2^2 - 2s_1s_2\cos\gamma = c^2$$

Still there is left one uncertainty.

Four or more markers determine the slant ranges fully.
R_2 and R_3 are common in both triangles.
And redundancy is eliminated.

Obtaining Angular Velocity Vector (1)

$$L_{inertia} = \Theta_t I \omega \tag{5}$$

The following discussion aims at finding $L_{inertia}$ or simply L vector as well as the inertia tensor I.

To this aim, first of all, here is introduced the manipulation of obtaining the angular velocity vector ω. The relation

$$\frac{dt_j}{dt} = \omega \times t_j \qquad t_j = X_j - X_4 \tag{4}$$

holds for the rigid body dynamics and discretization of

$$t_{j,t+1} = t_{j,t} + \omega \times t_j dt \tag{5}$$

It is expressed by the following relation.

$$\begin{bmatrix} t_1 & t_2 & t_3 \end{bmatrix}_{t+1} = \begin{bmatrix} t_1 & t_2 & t_3 \end{bmatrix}_t + [\hat{\omega}] \begin{bmatrix} t_1 & t_2 & t_3 \end{bmatrix}_t dt \tag{6}$$

This relation is expressed similarly to the cases more markers are observed. Using the relation of

$$T = \begin{bmatrix} t_1 & t_2 & t_3 \end{bmatrix}_t \quad \dot{T} = (\begin{bmatrix} t_1 & t_2 & t_3 \end{bmatrix}_{t+1} - \begin{bmatrix} t_1 & t_2 & t_3 \end{bmatrix}_t)/dt \tag{7}$$

the angular velocity vector expressed in the matrix form of

$$[\hat{\omega}] = \dot{T}T^{-1} \tag{8}$$

Note the number of columns in the matrix T may be larger than three. Inverse of T matrix can be generalized appropriately. The expected matrix should possess a skew property. However, the expression above does not guarantee it. In order to avoid the loss of the property, here is shown an alternative form as below.

$$[\hat{\omega}] = \frac{1}{2}(\dot{T}T^{-1} - (\dot{T}T^{-1})^{\mathrm{T}}) \tag{9}$$

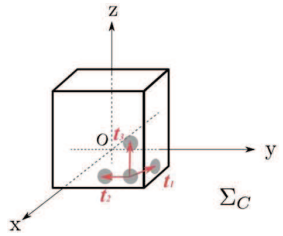

Fig.8 Vectors in camera-fixed coordinate

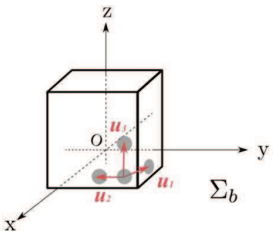

Fig.9 Vectors in body-fixed coordinate

Obtaining Angular Velocity Vector (2)

Note the number of columns in the matrix T may be larger than three. Inverse of T matrix can be generalized appropriately. To this aim, angular velocity should be sought to minimize the following criterion of

$$\mathrm{J} = \frac{1}{2} Tr. \left\{ \left[\dot{T} - [\omega] T \right] \left[\dot{T} - [\omega] T \right]^T \right\}$$

Requesting $\frac{\partial J}{\partial [\omega]} = 0$ concludes the general solution expressed as

$$[\hat{\omega}] = \left(\dot{T}T^T\right)(TT^T)^{-1}$$

Especially in case the number of columns of T is three, it reduces to eq. (8) above.

The expected matrix should possess a skew property. However, the expression above does not guarantee it. In order to avoid the loss of the property, here is shown an alternative form as below. The form is derived by another optimization criterion. Provided the matrix

$$[\hat{\omega}] = \frac{1}{2}(\dot{T}T^{-1} - (\dot{T}T^{-1})^{\mathrm{T}})$$

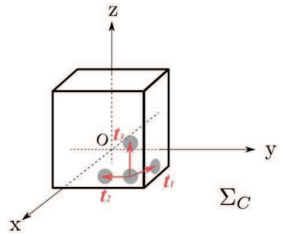

Fig.8 Vectors in camera-fixed coordinate

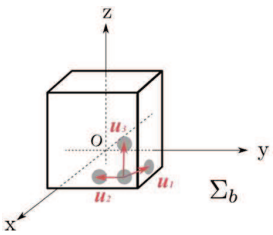

Fig.9 Vectors in body-fixed coordinate

Obtaining Angular Velocity Vector (3)

$[\hat{\omega}]$ is expected to be a skew symmetric matrix is near to a certain matrix A, the most probable solution is expressed via minimizing another optimization minimizing

$$J = \frac{1}{2} Tr.\left\{[[\omega] - A]^T [[\omega] - A]\right\} + S\{[\omega]^T + [\omega]\}$$

by introducing undetermined multiplier S. This concludes the most probable solution should take simply the form of:

$$[\hat{\omega}] = \frac{1}{2}(A - A^T)$$

This provides the expression of eq. (9)

$$[\hat{\omega}] = \frac{1}{2}(\dot{T}T^{-1} - (\dot{T}T^{-1})^{\mathrm{T}})$$

and generally

$$[\hat{\omega}] = \frac{1}{2}\{(\dot{T}T^T)(TT^T)^{-1} - (TT^T)^{-1}(T\dot{T}^T)\}$$

It automatically retains the skew property and the components of the angular velocity vector is retrieved legibly. It is obtained by optimizing the error in eq. (8) is minimized. Details are omitted

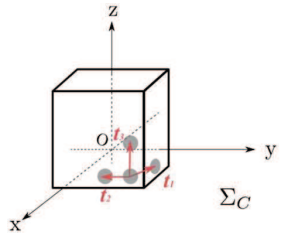

Fig.8 Vectors in camera-fixed coordinate

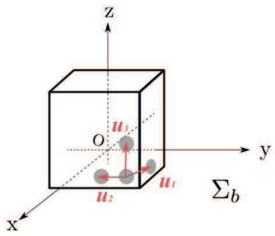

Fig.9 Vectors in body-fixed coordinate

Finding Coordinate Transformation Matrix (1)

Even in case the number of pairs in T and J exceeds three, the coordinate transformation matrix is sought to satisfy the augmented criterion as below.

$$J = \frac{1}{2} tr.[(T - \Theta J)^T (T - \Theta J)] + tr.\left[S\frac{1}{2}(\Theta^T\Theta - \mathbf{1})\right] \quad (13)$$

$$\Theta = \frac{1}{2}(TJ^T + JT^T)S^{-1} \quad (14)$$

When diagonalized into Λ^2 with the unitary matrix P as below,

$$\frac{1}{4}\left(TJ^T + JT^T\right)^2 = P\Lambda^2 P^T \quad (15)$$

The coordinate transformation P is obtained as a unitary matrix to diagonalize the symmetric matrix.

The multiplier S is determined as

$$S = P\Lambda P^T \quad (16)$$

And the coordinate transformation matrix is obtained as follows.

$$\Theta = \frac{1}{2}(TJ^T + JT^T)P\Lambda^{-1}P^T \quad (17)$$

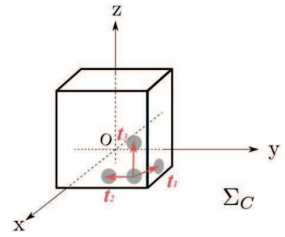

Fig.8 Vectors in camera-fixed coordinate

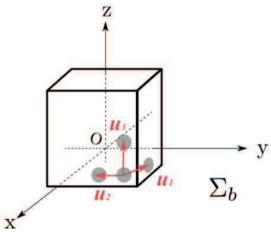

Fig.9 Vectors in body-fixed coordinate

$$J = [u_1 \quad u_2 \quad u_3]$$
$$T = \Theta J$$
$$\Theta = TJ^{-1}$$

Finding Coordinate Transformation Matrix (2)

Even in case the number of pairs in T and J exceeds three, the coordinate transformation matrix is sought still to satisfy the augmented criterion as below.

$$J = \frac{1}{2} tr.[(T - \Theta J)^T (T - \Theta J)] + tr.\left[S\frac{1}{2}(\Theta^T\Theta - \mathbf{1})\right] \quad (13)$$

The solution is expressed as the same as

$$\Theta = \frac{1}{2}(TJ^T + JT^T)P\Lambda^{-1}P^T \quad (17)$$

Here Θ matrix satisfies the unitary property and minimizes the discrepancy. It admits the inaccurate observation of the markers in T. Eq. (17) retains unitary property regardless of the scale of the markers' layout. It is the biggest difference from eq. (12).

In case, $J = kJ^*$, when J is scaled by a scalar k, the multiplier S is tuned automatically to make the unitary property associated with the matrix Θ, the solution eq. (17) remains unchanged.

This implies the size of J does not have to be prescribed. The target debris has only to carry a target / marker whose shape information is known.

The targets / markers can be rectangular plates such as the solar panels or the satellite hub panels whose edge ratio is known.

The shape information does not have to be prepared or delivered to the debris removal service at launch.

As long as the blue prints or drawings are available when the debris removal is requested for the satellite, the attitude information is obtained based on the images as described above.

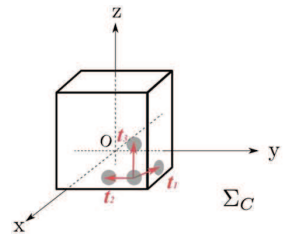

Fig.8 Vectors in camera-fixed coordinate

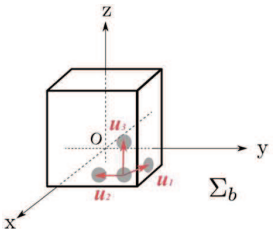

Fig.9 Vectors in body-fixed coordinate

$$J = [u_1 \quad u_2 \quad u_3]$$
$$T = \Theta J$$
$$\Theta = TJ^{-1}$$

Pose Estimation & DCM Solution Example

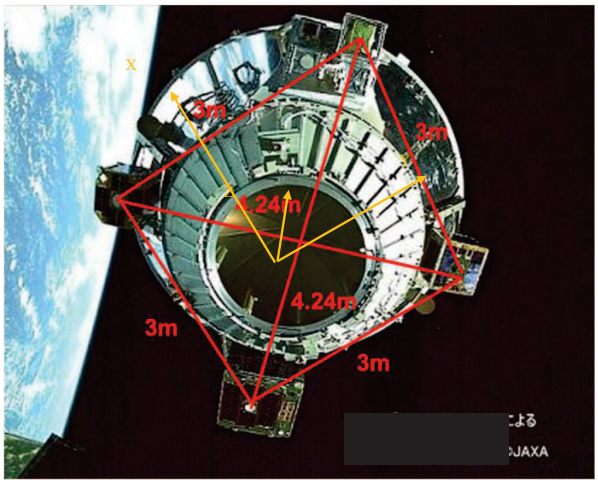

Fig.10 Disposed Upper Stage at Ibuki launch

The markers' position vectors on the camera-frame:

M1 = [209.40 686.61],

M2 = [-162.39 -556.98],

M3 = [-609.69 133.91],

M4 = [545.58 -115.38].

The positions of the four markers on the upper stage:

[1.5 1.5 -1.5,

-1.5 -1.5 -1.5,

-1.5 1.5 -1.5,

1.5 -1.5 -1.5]

The coordinate transformation matrix DCM (Direction Cosine Matrix) is obtained

$$DCM = \begin{bmatrix} 0.83244 & -0.43386 & -0.49813 \\ 0.49841 & 0.83646 & 0.086239 \\ 0.091411 & -0.3348 & -0.86098 \end{bmatrix}$$

When the Euler angles are (sequenced in yaw-pitch-roll order) used, they are

yaw = -27.53deg, pitch = 29.88deg, roll = 5.72deg respectively.

Angular Momentum Vector & Inertia Tensor Estimation (1)

$$J = \frac{1}{2}\sum_{k=1}^{N}\left\|\Theta_k^T L - I\widehat{\omega_k}\right\|^2 + \frac{1}{2}\mu(L^T L - 1) \quad (19)$$

The first term simply requests the total angular momentum vector transformed by I should be seen as a constant vector L. The second term requests the magnitude of L be a certain constant quantity. The quantity is taken here as one Nms (unit). I and L are proportional with each other.

The optimality condition on L concludes it be written as below.

$$L = \frac{1}{N+\mu}\sum_{k=1}^{N}(\Theta_k I\widehat{\omega_k}) \quad (20)$$

N denotes the number of observations. μ is determined to make the magnitude of L be unit. The optimality condition on I requests

$$\frac{\partial J}{\partial I} = \frac{1}{2}\sum_{k=1}^{N}\left(\widehat{\omega_k}\widehat{\omega_k}^T\right)I^* + \frac{1}{2}I^*\sum_{k=1}^{N}\left(\widehat{\omega_k}\widehat{\omega_k}^T\right) - \frac{1}{2}\sum_{k=1}^{N}\left(\Theta_k^T L\widehat{\omega_k}^T\right) - \frac{1}{2}\sum_{k=1}^{N}\left(\widehat{\omega_k}L^T\Theta_k\right) = 0 \quad (21)$$

With the definition of

$$\Omega = \sum_{k=1}^{N}\left(\widehat{\omega_k}\widehat{\omega_k}^T\right) \quad (22)$$

The optimal inertia tensor I^* should satisfy the following condition.

$$\Omega I^* + I^*\Omega = \sum_{k=1}^{N}\left(\Theta_k^T L\widehat{\omega_k}^T\right) + \sum_{k=1}^{N}\left(\widehat{\omega_k}L^T\Theta_k\right) \quad (23)$$

Slight modification presents the Lyapunov matrix equation which I^* should satisfy as below.

$$(-\Omega)I^* + I^*(-\Omega) + \left(\sum_{k=1}^{N}\left(I\widehat{\omega_k}\widehat{\omega_k}^T\right) + \sum_{k=1}^{N}\left(\widehat{\omega_k}\widehat{\omega_k}^T I\right)\right) = 0 \quad (24)$$

Angular Momentum Vector & Inertia Tensor Estimation (2)

$$L = \frac{1}{N+\mu}\sum_{k=1}^{N}(\Theta_k I\widehat{\omega_k}) \quad \rightleftharpoons \quad \Omega I^* + I^*\Omega = \sum_{k=1}^{N}\left(\Theta_k^T L\widehat{\omega_k}^T\right) + \sum_{k=1}^{N}\left(\widehat{\omega_k}L^T\Theta_k\right)$$

If I is assumed simply as a unit matrix, the left hand equation notes the angular momentum vector L direction is the averaged angular velocity vector history.

The inertia tensor estimate I^* is found to satisfy the right hand side Lyapunov equation.
It guarantees the solution I^* is obtained as a positive definite matrix.

The solution is obtained through a boot-strap type iteration.

Example: Fragmentation

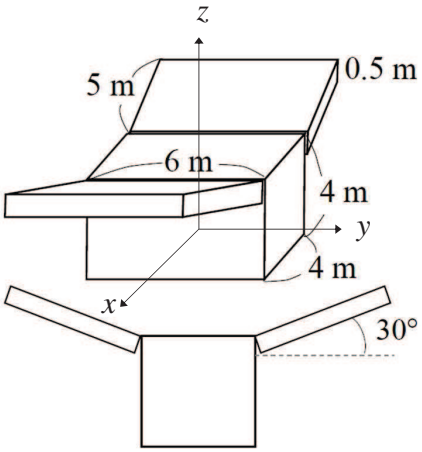

Fig.15 Model object spacecraft

$$I' = \begin{bmatrix} 2063 & 0 & 0 \\ 0 & 2580 & -324 \\ 0 & -324 & 2759 \end{bmatrix}$$

$\omega_{t=0}$ (0.0, 1.58, 4.74) deg/s,
$\Theta_{t=0}$ (π /4, π /4, π /3).

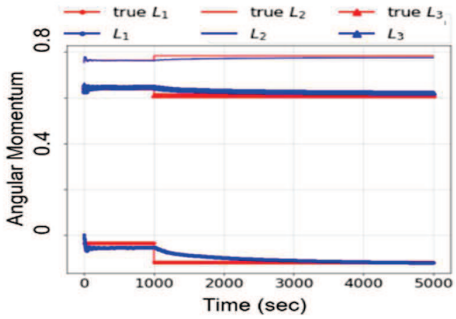

Fig. 16 Angular Momentum Vector

The normalized eigen values of I' is 11.6, 10.4, 9.7.

All the measurements are used for the batch estimation.
And the convergence is slow.

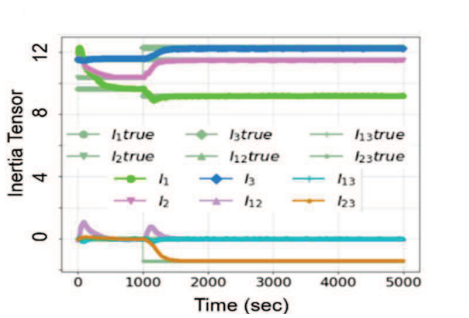

Fig. 17a Inertia Tensor

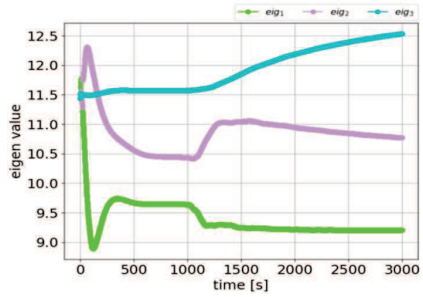

Fig. 17b Principal Moment of Inertia

Example: Direct Contact to cause Another Coning Motion

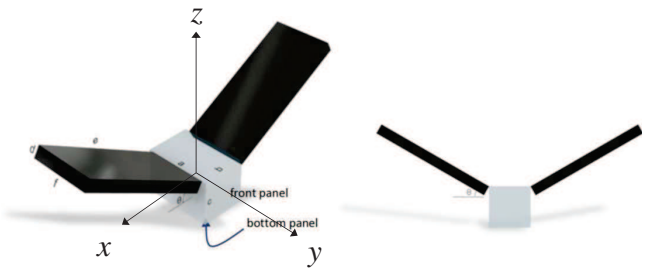

Fig.18 Spacecraft model for Case-3

Dimensional moment of inertia here is 506. 537, 573 kgm^2.
Initial angular velocity is 3deg/s for three axes.
And normalized inertia tensor is estimated proportionally.
Up to 1,200 data are used for each batch estimation.
Inertia tensor becomes correct around time=2,200sec.

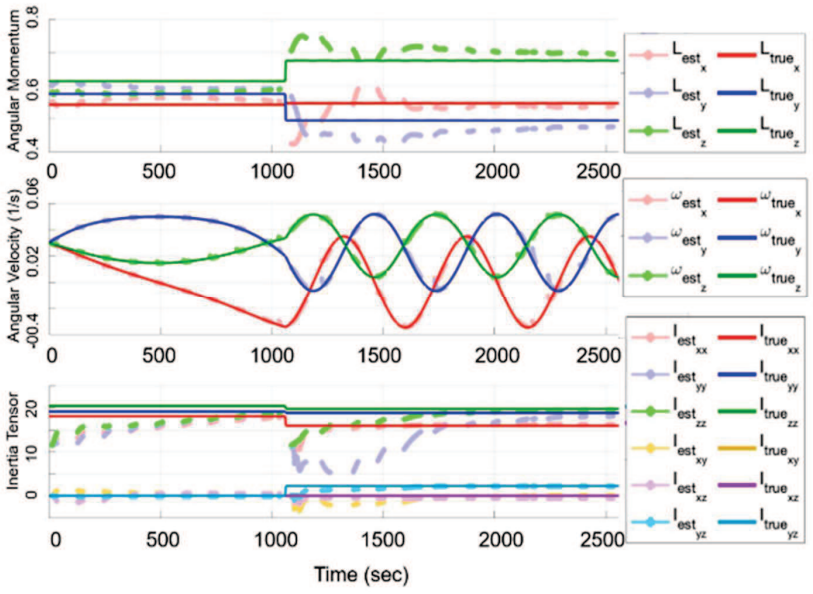

Fig. 19 Angular Momentum, Angular Velocity, Inertia Tensor – Contact Excitation on the Way

Conclusion

- Despite a large number of researches for decades, the motion estimation especially the angular momentum vector estimation has not been well solved, while it is critical in accessing uncooperative targets.
- The key problem in approaching to the target is in finding the frozen direction, the angular momentum vector.
- However, identifying the vector requires / accompanies the estimation of the inertia tensor matrix of the target.
- The linearized filters do not function well. In the practical applications, inertia principal axes may largely differ from the geometric axes, and the contact may cause another coning motion.
- A key outcome is the batch process for estimating the inertia tensor without relying on the nominal a priori parameters and the reference trajectories for the state variables.
- It works as the recursive and successive update process and is enough robust in real applications. No a priori parameters are required.
- The scheme never requests the prescribed targets onboard the potential targets at launch and allows the size very flexibly. The only information associated with the targets is the shape, which should provide the multiple markers more than three, four or more.